International Journal of Engineering, Mathematical and Physical Sciences
ISSN: 2517-9934
Vol:8, No:1, 2014

Native Point Defects in ZnO

A. M. Gsiea, J. P. Goss, P. R. Briddon, Ramadan. M. Al-habashi, K. M. Etmimi, Khaled. A. S. Marghani

Abstract—Using first-principles methods based on density functional theory and pseudopotentials, we have performed a details study of native defects in ZnO. Native point defects are unlikely to be cause of the unintentional n-type conductivity. Oxygen vacancies, which considered most often been invoked as shallow donors, have high formation energies in n-type ZnO, in edition are a deep donors. Zinc interstitials are shallow donors, with high formation energies in n-type ZnO, and thus unlikely to be responsible on their own for unintentional n-type conductivity under equilibrium conditions, as well as Zn antisites which have higher formation energies than zinc interstitials. Zinc vacancies are deep acceptors with low formation energies for n-type and in which case they will not play role in p-type coductivity of ZnO. Oxygen interstitials are stable in the form of electrically inactive split interstitials as well as deep acceptors at the octahedral interstitial site under n-type conditions. Our results may provide a guide to experimental studies of point defects in ZnO.

Keywords—DFT, Native, n-Type, ZnO.

I. Introduction

EXPERIMENTALLY, there is no conclusive evidence regarding a dominant role for native defects in as-grown ZnO[1], [2], [3], [4]. However, calculations of diffusion of native defects, their anticipated impact upon electrical conductivity and Hall Effect measurements, may be combined and viewed as evidence that native defects are the dominant defects causing unintentional electrical conductivity in as-grown ZnO. Regardless of their role in electrical conduction, photoluminescence observations of bulk ZnO commonly show green and blue luminescence, both of which have been widely attributed to native defects [5], [6], [7]. Understanding the behaviour of native defects is critical to the successful application of any semiconductor material, especially in compound materials. These defects often affect, directly or indirectly, the doping efficiency, growth of the material, and subsequent device specification. Oxygen vacancies, V_O, zinc interstitials, Zn_i, oxygen interstitial, O_i, and zinc vacancies, V_{Zn} are the primitive forms of native defects in ZnO. Oxygen vacancies and zinc interstitials have been suggested as the source of the commonly observed unintentional n-type conductivity in as-grown ZnO, while oxygen interstitials and zinc vacancies are potential sources of p-type ZnO [8], [9], [10]. Perhaps more importantly in the context of intentional doping with impurities, there is a significant possibility that combinations of dopants with native defects may affect conduction mechanisms. It is critical to have a good understanding of the structure and electronic properties of these native defects so that their interaction with dopants can be viewed in a broader context.

A. M. Gsiea is with Faculty of Science, Physics Department, Azzaytuna University, Libya. (e-mail: abslam_68@yahoo.com).
J. P. Goss, P. R. Briddon are with the Department of Electrical, Electronic and Computer Engineering, Newcastle Upon Tyne, England.
hpashy. R is with Faculty of Science, Physics Department, Azzaytuna University, Libya.
K. M. Etmimi, Khaled. A. S. Marghani are with Faculty of Science, Physics Department, Tripoli University, Libya.

II. Method

We use density-functional theory within the AIMPRO package[11], [12]. Defects are simulated within large super-cells containing 192 host-atoms, comprised from $(4 \times 4 \times 3)$ primitive cells. We use the calculated equilibrium lattice constants of $a = 6.18$ Å and $c = 9.81$ Å, respectively, which are in good agreement with experiment. The Brillouin-zone is sampled using the Monkhorst-Pack[13] scheme with a mesh of $2\times2\times2$ k-points. Structures are optimized via a conjugate-gradients scheme until the change in energy between iterations is less than 10^{-5}Ha, and forces are below 10^{-3}a.u. Atoms are simulated using *ab initio* pseudo potentials[14] and the total energies and forces are obtained with a local density approximation for the exchange-correlation[15]. The wave functions and charge density are expanded in terms of Gaussian orbitals and plane-waves, respectively[16]. For the Zn, and O impurities we include s, p and d functions, with a total of 28, 28 and 32 functions per atom, respectively. Matrix elements of the Hamiltonian are determined using a plane wave expansion of the density and Kohn-Sham potential [17] with a cutoff of 150 Ry, yielding well converged total energies with respect to the charge density basis. We calculate the formation energy of a defect X using

$$E^f(X,q) = E^{\rm tot}(X,q) - \sum_i \mu_i + q\mu_e + \chi(X,q) \qquad (1)$$

where $E^{\rm tot}(X,q)$ is the total energy of system X in charge state q. μ_i denotes the chemical potential of atomic species, $E_v(X,q)$ is the Fermi energy at the valance-band top, μ_e is the electron chemical potential, defined as zero at the valence band top, and $\chi(X,q)$ is a correction term to compensate for artifacts of the boundary conditions. In ZnO, the chemical potentials of components $\mu_{\rm O}$ and $\mu_{\rm Zn}$ are related by $E({\rm ZnO}) = \mu_{\rm O} + \mu_{\rm Zn}$ where $E({\rm ZnO})$ is the energy per bulk formula unit in ZnO. The range of possible values for $\mu_{\rm O}$ and $\mu_{\rm Zn}$ is related to the requirement for ZnO to be stable relative to decomposition into its elemental constituents, so that the zinc-rich limit is taken from zinc-metal, and for oxygen-rich limit $\mu_{\rm O}$ is taken from the O_2 molecule. The heat of formation for ZnO in this way is calculated to be 3.9 eV, while experimentally it is 3.61eV[18]. Relative formation energies per impurity atom are independent of the impurity chemical potential.

For the electrical characteristics of the defect centers, we calculate the transition levels, $E(q, q')$, defined as the electron chemical potential where the formation energies for two charge states, q and q', are equal. The effect upon the electrical levels arising from the periodic boundary condition, $\chi(X, q)$ in Eq. 1, is a complicated and controversial quantity to estimate. In this study, we have adopted a simple approach as we are focusing on the larger differences between the formation energies of different structures, rather than the specific values of the donor and acceptor levels. We correct the total energies using the Lany and Zunger model[19], and to take into account the underestimation of the band gap we also add a term proportional to the number of electrons in a conduction-band-like level[20], [21] of 2 eV per electron arising from a simple addition of the difference between the calculated and experimental band-gaps. The calculated electrical levels should be regarded as having error bars due to uncertainties in the calculation of the energies and correction terms of the order of a few 10ths of an eV. When comparing the absolute formation energies, and in particular in the important cases of comparison between like-systems, such as band-like donors, or comparison between the models for p-type doping, the corrections largely cancel. Then the energy differences between two donor systems, or two acceptor systems are generally accepted to be reasonably reliable at a quantitative level.

III. Results

A. The oxygen Vacancy, V_O

Based upon simple ionic arguments, the native defect V_O might well be expected to be a source of compensation in p-type ZnO doped with group-V impurities. V_O may be envisaged as a host oxygen atom, in the -2 oxidation state, being removed from the lattice. The electrons that would normally be bound to the now missing O atom can be viewed as coming from the four neighbouring Zn sites, half an electron from each. These electrons are still present, at least for an uncharged defect, so the two additional electrons that would have been at the O site mean that V_O is expect to act as a (double) donor. Fig. 1 shows the relaxed structure of V_O. In the neutral charge state the four neighbouring Zn atoms shift inwards by around 10%, forming a pair of Zn–Zn bonds. In the case of the +1 and +2 charge states, the four neighbouring Zn atoms shift in the opposite direction, i.e. breathe outwards by 3% and 23% respectively. The structures obtained using AIMPRO are in excellent agreement with other theoretical studies [23], [22], [20]. The origin of the different structures may be viewed as a chemical reconstruction in the neutral charge state, and this large geometric effect has an impact upon the electrical properties. The charge-dependent formation energies (Fig. 2) indicate a (0/+2) level around $E_v + 1.0$ eV, too deep for the production of n-type ZnO. The oxygen vacancy is a deep, negative-U donor, where the 1+ charge state is never thermodynamically the most stable charge state for any value of the electron chemical potential. Then, when the Fermi energy is above the $(0/+2)$ level, the defect is in the neutral charge state. When the Fermi energy is below

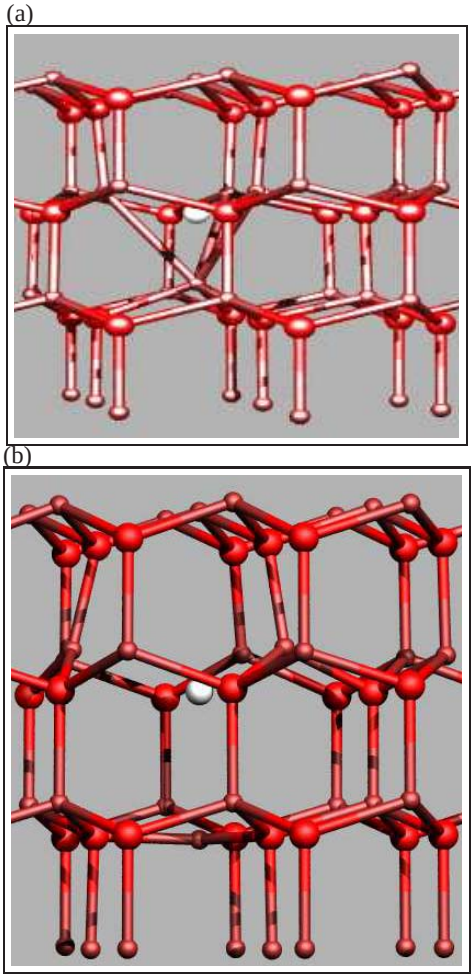

Fig. 1. Schematics of V_O in (a) the neutral charge state, and (b) the positive (+2) charge state. Red and brown Colours indicated oxygen and zinc atoms, respectively. The white circles indicate the vacated oxygen sites. Vertical and horizontal axes are [0001] and [0110] directions, respectively.

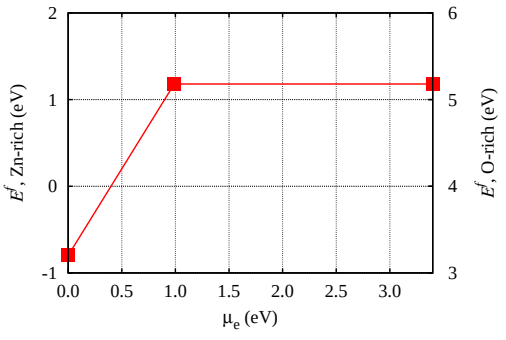

Fig. 2. Plot of E^f *vs.* μ_e for V_O in ZnO calculated using the 192 atom supercell.

the $(0/+2)$ level, the defect has a charge of $+2e$. The negative-U nature of this centre is a result of the chemical reconstruction in the neutral charge state: indeed, negative-U

centres are typically characterised by large structural changes with charge state. It is noted that, in addition to the structural agreement, the donor level is in excellent agreement with the transition level of $E_v + 1.0\,\mathrm{eV}$ of previous calculations [24], [25], [26]. The current calculation indicates that neutral V_O has a relatively low formation energy of $\sim 1\,\mathrm{eV}$ under Zn-rich conditions, which is in good agreement with other theoretical calculations [25], [26], [27], [28]. In addition, the formation energy is lower in p-type ZnO. This is consistent with the model that under such conditions, V_O centres are formed during growth, compensating the acceptor species and preventing the formation of highly conductive material. It is worth noting that previous calculations suggest that V_O has relatively high migration barrier of 2.4 eV [20]. This would imply that V_O undergoes little diffusion at room temperature, but that annealing to higher temperatures may result in the movement of these double donors, and possibly their direct interaction with other defects in the lattice, such as candidate acceptors.

B. Zinc Interstitial Zn_i

Zinc interstitials might, in principle, be another of the sources of the common, unintentional n-type conductivity in as-grown ZnO. It is understood that there are two main sites for zinc interstitials in the Wurtzite structure: Zn_i at the tetrahedral interstitials site, $Zn_i,\ \mathrm{tet}$ as shown in Fig. 3(a), and zinc at the octahedral interstitial site, $Zn_i,\ \mathrm{oct}$, as shown in Fig. 3(b). The difference between the tetrahedral and octahedral interstitial sites can be understood by considering a view of the Wurtzite structure along the hexagonal axes. There are open, six-member channels in the structure, and a location within one such channel approximately equidistant from six oxygen sites is the octahedral interstitial location. In contrast, the tetrahedral location is along a c-axis column occupied by host atoms, so that viewed along the hexagonal axis, the tetrahedral site is eclipsed by host atoms. In fact the tetrahedral site can be viewed as a site along the c-axis projected from a host site away from the associated host bond, such that it is approximately equidistant from four host oxygen atoms. It is found that $Zn_i,\ \mathrm{oct}$ is more stable than $Zn_i,\ \mathrm{tet}$ by 1.2 eV, in the +2 charge state, which is in reasonable agreement with previous calculations for this defect centre [20]. Placing the zinc interstitial at an octahedral site induces a noticeable local lattice relaxation, particularly in terms of a strong interaction between the Zn atom and three of the nearest neighbour O atoms. For the additional Zn ion, the six surrounding Zn atoms are moved outward by 0.2Å, the ionic Zn_i-Zn bond distance being calculated to be between 2.36Å and 2.73Å. This is smaller than the value of 2.66Å and 2.81Å for bulk Zn metal (which is hcp in structure and therefore has neighbours at different distances). Zn interstitials have a relatively high formation energy in n-type material and are expected to rapidly diffuse with a low migration barrier of about $0.57\,\mathrm{eV}$ [20]. The charge-dependent formation energies in the current calculations, plotted in Fig. 4, indicate a (0/+2) level above the conduction-band minimum).

It is therefore found that the zinc interstitial behaves a shallow donor, which is in agreement with the interpretation

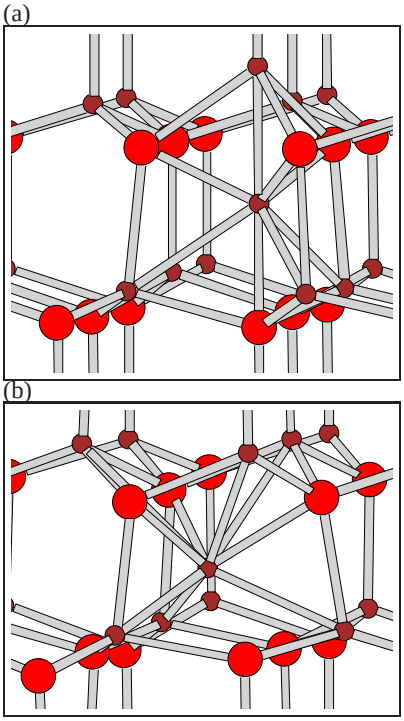

Fig. 3. Schematics of Zn_i in ZnO (a) at tetrahedral site $Zn_i,\ \mathrm{tet}$ (b) octahedral site $Zn_i,\ \mathrm{oct}$. Colours and axis are as in Fig. 1.

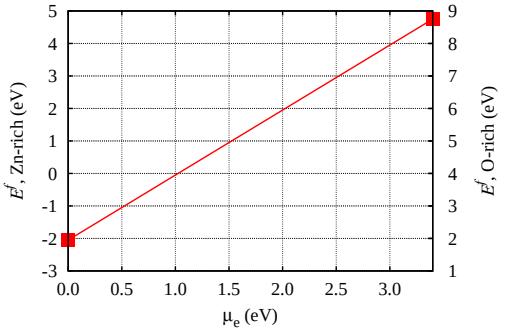

Fig. 4. Plot of E^f *vs.* μ_e for Zn_i defects in ZnO calculated using the 192 atom supercell.

of some experimental observations [2], [29], although its thermodynamic stability might well be questioned. Based upon the calculated energy of formation and migration barrier, Zn interstitials are not expected to be stable in pure ZnO at room temperature [30], and are thus unlikely to be responsible on their own for unintentional n-type conductivity under equilibrium conditions. On the other hand, the zinc interstitial can diffusion relatively freely due to its low barrier, and thus may cause it to find other sites such as V_O to form Zn_O or be attracted Coulombically to with negatively charged impurities which can form a complex with sufficiently high binding energy. This interaction may provide a mechanism to play a role in the unintentional n-type conductivity of ZnO.

C. Oxygen Interstitial O_i

As with the zinc interstitial, there are two type of non-bonded oxygen interstitial O_i sites in the w-ZnO: O_i at tetrahedral O_i, tet or octahedral site O_i, oct. It is found in these calculations that O_i, tet is unstable and relaxes into a split-interstitial configuration as shown in Fig. 5(a), $(O_2)_O$. In this case, the O-O bond length was calculated as

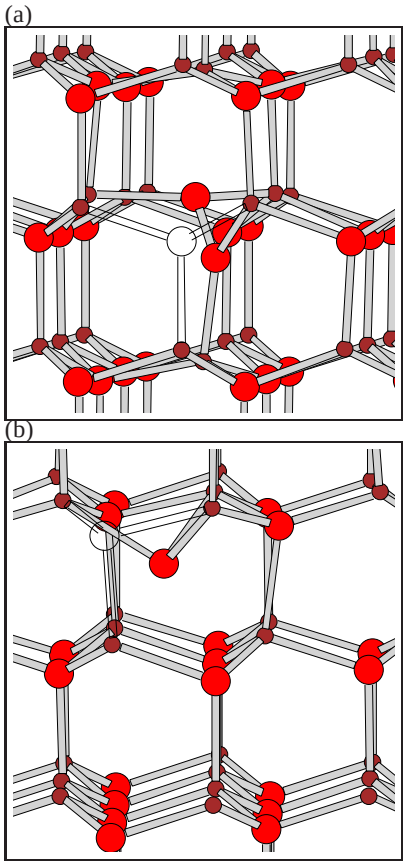

Fig. 5. Schematics of O_i in ZnO (a) starting from the tetrahedral site O_i, tet, and (b) the octahedral site O_i, oct. Colours and axis are as in Fig. 1. Atoms and bonds that would otherwise obscure the structure of the interstitials are shown in outline for the sake of clarity.

1.46Å, which is in good agreement with other theoretical calculations 1.46Å [22], and the experimental value of 1.49Å for gas phase O_2^{2+}. Oxygen at the octahedral site O_i, oct is shown in Fig. 5(b), which introduces states in the band-gap that could accept two electrons. For the neutral charge state the total energy for O_i, oct is higher by 1.66 eV than that of the $(O_2)_O$, while O_i, oct site is lower in energy for negative charge states. This is in good agreement with other theoretical calculations [20], [31], [9]. The Zn-O_i, oct distance calculated to be 2.19Å, somewhat greater than the 1.98Å for the host Zn–O bond-length. The charge-dependent formation energies, Fig. 6, indicate a (0/+1) level around $E_v + 0.3$ eV, and therefore will not contribute to n-type conduction in ZnO. The electrical level of the split-interstitial are derived from anti-bonding $pp\pi^*$ state from a molecular orbital of the isolated O_2 molecule. This explains the O–O

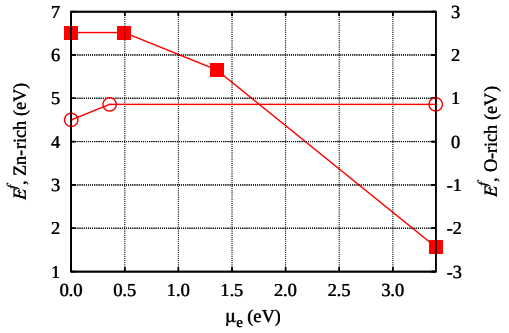

Fig. 6. Plot of E^f *vs.* μ_e for O_i, oct (■), O_i, tet (O). The energy is calculated using the 192 atom supercell.

bond length for split interstitial which longer than the O_2 molecule. Oxygen at the octahedral site introduces states in the band-gap that can accept two electrons, so transition levels of O_i, oct (0/−1) and (−1/−2) are located at 0.5 eV and 1.4 eV above the valance-band maximum, respectively. These levels are derived from the empty partially $2p$ orbitals of O_i. Previous calculations have determined that oxygen interstitials have a relatively low migration barrier: 0.9 eV for O_i^0 (split) and 1.1 eV for O_i^{2-} (oct) [20]. If such species are present in the material, they may reduce the concentration of V_O donors even at modest temperatures. Alternatively they may be electrostatically attracted to impurities and form a complex with, for example, group-V elements. This interaction may provide a mechanism to play a role in the p-type conductivity of ZnO [32].

D. Zinc Vacancy V_{Zn}

The relaxed structure of V_{Zn} for the neutral charge state is shown in Fig. 7(a). The oxygen atoms around the zinc vacancy shift outward by about 3% with respect to the equilibrium ZnO bond length. For the negative charge state, $(V_{Zn})^{-1}$, there is a similar relaxation. However, for $(V_{Zn})^{-2}$ there is a much more substantial relaxation. Based upon the location of the ideal site of the zinc at that has been removed, in the fully ionised form the the 'V–O' distance is calculated to be 1.98Å in the a,b-plane, but 2.57Å in c-direction, as shown in Fig. 7(b). Fig. 8 shows a plot including the formation energies (Eq.1) of V_{Zn} in ZnO. This yields a double acceptor level, in line with previous calculations [35], [31], [20], [34]. The (0/−1) transition level is located around $E_v + 0.1$ eV and the (−1/−2) transition level around $E_v + 0.6$ eV above the valance band top, both of which are also in good agreement with other theoretical calculations [31], [20], [33]. Neutral V_{Zn} centres have a very high formation energy, being about 3.5 eV in the neutral charge state even under under O-rich conditions. In n-type material the formation energy is lower. However, the equilibrium concentration might be expected to be low, and in which case they will not play a role in p-type conductivity of ZnO, as sometimes has been suggested [36], [37], [21].

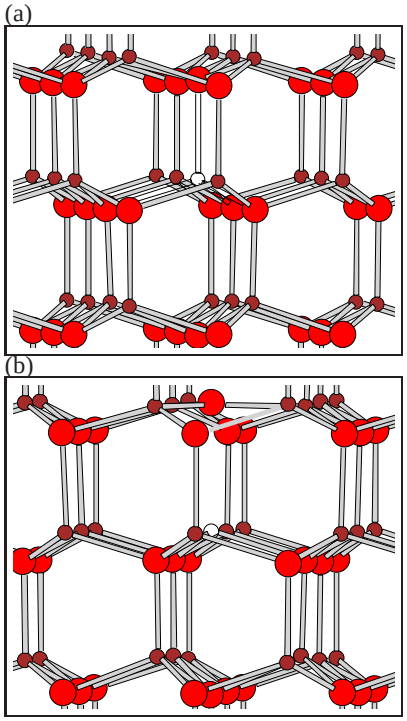

Fig. 7. Schematics of V_{Zn} in ZnO (a) at neutral charge state (b) in (-2) charge state. Colours and axis are as in Fig. 1.

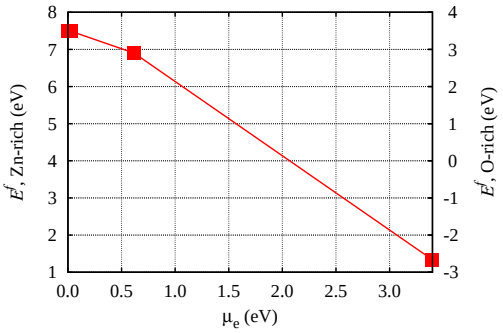

Fig. 8. Plot of E^f *vs.* μ_e for V_{Zn} defect in ZnO. The energy is calculated using the 192 atom supercell.

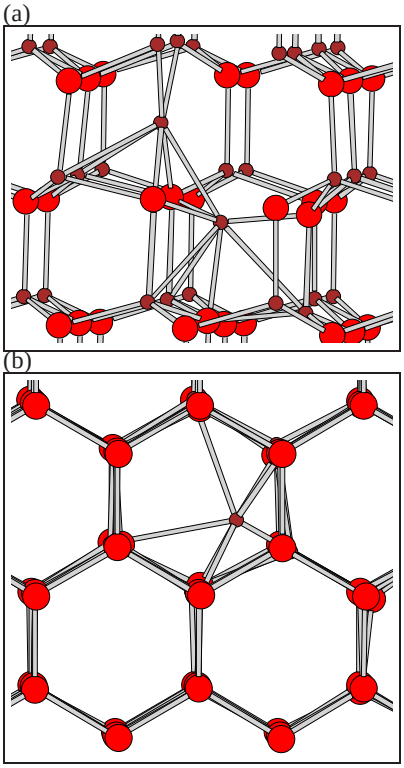

Fig. 9. Schematics of Zn_O in ZnO. Colours are as in Fig. 1. (a) and (b) show views along [2 1 1 0] and along the hexagonal axis, respectively.

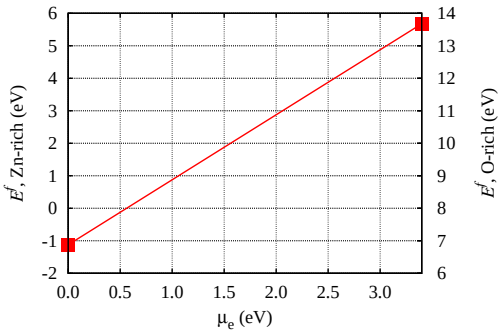

Fig. 10. Plot of E^f *vs.* μ_e for Zn_O. The energy is calculated using the 192 atom supercell.

E. Zinc Antisite Zn_O

Finally, the zinc antisite defect is reviewed. This consists of a zinc atom substituting for an oxygen host atom. The relaxed structure of Zn_O for the +2 charge state is shown in Fig. 9. After optimisation, in the +2 charge state structure the Zn_O–O distance is calculated to be 2.20Å, which is larger than the host Zn–O bond length by about 10%. As ZnO is a hexagonal material, there are two different Zn_O–Zn distances: three Zn_O–Zn distances are calculated to be 2.4Å, and another two Zn_O–Zn distance of 2.80Å. These values are in good agreement with other theoretical calculations [22], [20]. Fig. 10 shows a plot of the formation energies (Eq.1) of Zn_O in ZnO. Only the +2 charge state is thermodynamically stable in the band-gap. Perhaps more significantly, although the zinc antisite has a high formation energy in n-type, O-rich material, they would be highly favourable in Zn-rich, p-type material. Such centres, being shallow double-donors must be considered to be a plausible compensation centre.

IV. Conclusion

To facilitate comparison between the various forms, the results of the formation energies for native defects are summarised in Fig 11. As one might expect, in oxygen-rich material, V_{Zn} and O_i centres dominate. Both act as acceptors,

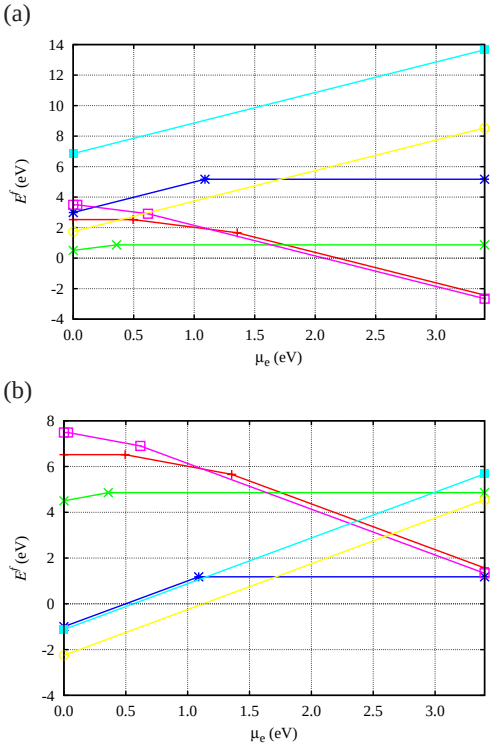

Fig. 11. Plot of E^f *vs.* μ_e for the native defects for ZnO. The energy is calculated using the 192 atom supercell: V_O(∗), O_i(split)(x), O_i(Oct)(+), Zn_i(Oct)(O), Zn_O(■), V_{Zn}(□). (a) Oxygen-rich conditions (b) Zinc-rich conditions

but as O_i can chemically react with the lattice to form covalent bonds with host oxygen, this can also be a donor. Under equilibrium conditions, a combination of O_i and V_{Zn} would be expected to yield compensated material. The chemistry resulting in the covalent bond in the neutral charge state of O_i is an important qualitative effect that shall be seen to be significant in the case of impurity doping. In Zn-rich material, V_O, Zn_i and perhaps surprisingly, the Zn antisite is favoured. All of these centres are donors, but in the cases of the antisite and Zn_i the donor levels are shallow. Although it is inadvisable to rely upon these energies exclusively, the calculations here, and from previous reports, are consistent with the potential role for native defects as shallow donors to generate n-type conductivity in as-grown material.

References

[1] N. S. Han, H. S. Shim, , J. H. Seo, S. Y. Kim, S. M. Park, and J. K. Song, J.Appl. Phys. **107**, 084306 (2010).
[2] D. C. Look, J. W. Hemsky, and J. R. Sizelove, Phys. Rev. Lett. **82**, 2552 (1999).
[3] C. G. Van de Walle, Phys. Rev. Lett. **85**, 1012 (2000).
[4] L. S. Vlasenko, G. D. Watkins, and R. Helbig, Phys. Rev. B. **71**, 115205 (2005).
[5] T. Kondela, Gregus. D. Zahoran, and T. Roch, Mat. Sci. Eng. **15**, 012041 (2010).
[6] K. Vanheusden, C. H. Seager, W. L. Warren D. R. Tallant and J. A. Voigt, Appl. Phys. Lett. **68**, 403 (1969).
[7] D. C. Reynods, D. C. Look, and B. Jogai, J. Appl. Phys. **89**, 6189 (2001).
[8] C. G. Park, S. B. Zhang, and S.-H. Wei, Phys. Rev. B. **66**, 073202 (2002).
[9] E. C. Lee Y. S. Kim, Y. G Jin, and K. J. Chang, Phys. Rev. B. **64**, 085120(2001).
[10] S. Limpijumnong, and S. B. Zhang, Appl. Phys. Lett. **86**, 151910 (2005).
[11] P. R. Briddon and R. Jones, Phys. Status Solidi B **217**, 131 (2000).
[12] M. J. Rayson and P. R. Briddon, Computer Phys. Comm. **178**, 128 (2008).
[13] H. J. Monkhorst and J. D. Pack, Phys. Rev. B. **13**, 5188 (1976).
[14] N. Troullier and J. L. Martins, Phys. Rev. B. **43**, 1993 (1991).
[15] J. P. Perdew and Y. Wang, Phys. Rev. B. **45**, 13244 (1992).
[16] J. P. Goss, M. J. Shaw, and P. R. Briddon, in *Theory of Defects in Semiconductors*, Vol. 104 of *Topics in Applied Physics*, edited by David A. Drabold and Stefan K. Estreicher (Springer, Berlin/Heidelberg, 2007), pp. 69–94.
[17] M. J. Rayson and P. R. Briddon, Phys. Rev. B. **80**, 205104 (2009).
[18] *CRC handbook of chemistry and physics*, 73 ed., edited by D. R. Lide (CRC, Boca Raton, FL, 1992).
[19] S. Lany and A. Zunger, Phys. Rev. B. **78**, 235104 (2008).
[20] A. Janotti and C. G. Van de Walle, Phys. Rev. B. **76**, 165202 (2007).
[21] W. -J Lee J. Kang, and K. J. Chang, Phys. Rev. B. **73**, 024117 (2007).
[22] A. Janotti and C. G. Van de Walle, J. Cryst. Growth. **287**, 58 (2007).
[23] E. C Lee, Y. G. Chang, K. J. Kim, and Y. S. Jin, Phys. B. **73**, 024117 (2007).
[24] C. D. Pemmaraju, R. Hanafin, T. Archer, H. B. Braun, and S. Sanvito, Phys. Rev. B. **78**, 054428 (2008).
[25] P. Erhart, K. Albe, and A. Klein, Phys. Rev. B. **73**, 205203 (2006).
[26] Stephan. Lany, and Alex. Zunger, Phys. Rev. Lett. **98**, 045501 (2007).
[27] S. Lany, and A. Zunger, Phys. Rev. B. **78**, 235104 (2008).
[28] F. Oba, I. Togo, A. Tanaka, J. Paier, and G. Kresse, Phys. Rev. B. **77**, 245202 (2008).
[29] A. R. Hutson, Phy. Rev. **108**, 222 (1957).
[30] P. Erhart, and K. Albe, Appl. Phys. Lett. **88**, 201918 (2006).
[31] A. F. Kohan, G. Ceder, D. Morgan, and C. G. van de Walle, Phys. Rev. B. **61**, 15019 (2000).
[32] A. M. Gsiea, J. P. Goss, P. R. Briddon, and K. M. Etmimi, W. A. S. T. **75**, 576 (2013).
[33] M. G. Wardle, J. P. Goss, and P. R. Briddon, Phys. Rev. B. **72**, 155108 (2005)
[34] M. G. Wardle, J. P. Goss, and P. R. Briddon, Phys. Rev. B. **71**, 155205 (2005)
[35] S. Limpijumnong, S. B. Zhang, Su-Huai. Wei, and C. H. Park, Phys. Rev. Lett. **92**, 1555041 (2004).
[36] R-Y. Tian, and Y-J. Zhao, J. Appl. Phys. **106**, 043707 (2009).
[37] X. Xu, Y. Shen, N. Xu, W. Hu, J. Lai, and J. Ying, Z. Wu, Vacuum **48**, 1306 (2010).